Approximate Message Passing Algorithms for Low Complexity OFDM-IM Detection

Zeping Sui, *Student Member, IEEE*, Shefeng Yan, *Senior Member, IEEE*, Hongming Zhang, *Member, IEEE*, Lie-Liang Yang, *Fellow, IEEE*, and Lajos Hanzo, *Fellow, IEEE*

***Abstract*—Low complexity approximate message passing (AMP) orthogonal frequency division multiplexing combined with index modulation (OFDM-IM) detection algorithms are proposed, which exploit the sparse structure of the frequency domain (FD) OFDM-IM symbols. To circumvent the high root mean square error (RMSE) in the conventional AMP algorithm, a minimum mean square error (MMSE) denoiser is proposed based on the classic Bayesian approach and on the state evolution of AMP. Our simulation results demonstrate that it is capable of improving both the RMSE as well as the convergence rate. However, in practice, the channel's diagonal FD matrix may be a non-Gaussian sensing matrix, hence a damping strategy is conceived. In conclusion, the proposed MMSE denoiser based damping-assisted AMP-aided detector strikes a compelling bit error ratio vs. complexity trade-off.**

***Index Terms*—OFDM, index modulation (IM), MMSE, compressed sensing (CS), approximate message passing.**

I. Introduction

Orthogonal frequency division multiplexing (OFDM) combined with index modulated (OFDM-IM) has been regarded as a competitive candidate for next-generation systems [1], [2]. As a benefit, OFDM-IM systems are capable of striking a flexible trade-off between SE and energy efficiency (EE), while reducing both the peak-to-average ratio (PAPR) and bit error ratio (BER) of classical OFDM [3], [4].

Since the performance of OFDM-IM is dependent on the amplitude-phase modulated (APM) symbols and the subcarrier activation patterns (SAPs), it is crucial to design joint APM and IM detectors having a low complexity [5]–[7]. By exploiting the fact that the frequency-domain symbols (FD) in OFDM-IM may either be zero or non-zero, a reduced-complexity log-likelihood ratio detector (LLRD) has been proposed in [8]. Then later a low-complexity greedy detection algorithm was proposed for multicarrier index keying (MCIK) [9]. Furthermore, inspired by the conception of greedy pursuit, a low-complexity detector based on iterative residual checking (IRC) has been conceived, where locally optimal estimates are obtained at each iteration [2]. Additionally, based on the above-mentioned compressed sensing (CS) algorithms, a low-complexity generalized iterative residual checking aided detector (GIRCD) was proposed in [10].

As a further advance, it has been shown that the approximate message passing (AMP) algorithm has the advantages of low-complexity and fast convergence [11]. Then a generalized approximate message passing (GAMP) detector has been proposed in [12]. Later in [4], Zhang *et al.* proposed an AMP-assisted detector for OFDM-IM using single subcarrier activation for improving the system performance.

By exploiting the statistics of the frequency domain (FD) OFDM-IM symbols, we conceive low-complexity minimum mean square error (MMSE) denoiser based AMP detectors for OFDM-IM systems. Our new contributions are boldly and explicitly contrasted to the existing solutions in Table I at a glance, which are also detailed as follows:

- We propose a computationally efficient AMP-aided detector by specifically designing the MMSE denoiser for OFDM-IM, which is referred to as the MMSE denoiser based damping-assisted AMP detector (MMSE-DAMPD). We first introduce a conventional AMP-aided detector by exploiting the sparsity of the received FD symbols. Then, based on the state evolution of the AMP algorithm, a sophisticated MMSE denoiser is proposed relying on the powerful Bayesian approach by exploiting the statistics of the FD symbols. Furthermore, we conceived a novel damping strategy for improving the convergence of the AMP algorithm as and when the measurement matrix does not obey the zero-mean independent and identically distributed (i.i.d.) Gaussian distribution.
- The root mean square error (RMSE) performance of the AMP detector relying on soft thresholding denoiser [13] and that using an MMSE denoiser is compared for different SAPs vs. the signal-to-noise ratio (SNR). It is demonstrated that the proposed MMSE denoiser is capable of achieving lower RMSE and faster convergence. Furthermore, the BER performance of MMSE-DAMPD-aided OFDM-IM systems is evaluated at different throughput values, showing that the proposed detector is capable of striking an attractive BER vs. complexity trade-off.

The rest of the paper is organized as follows. In Section

This work was supported by the the National Science Foundation of China under Grants 61725106 and 62001056 and the China Scholarship Council under Grant 202004910653. (*Corresponding author: Shefeng Yan*)

Zeping Sui and Shefeng Yan are with the Institute of Acoustics, Chinese Academy of Sciences, Beijing 100190, China, and also with the University of Chinese Academy of Sciences, Beijing 100049, China (e-mail: suizeping@mail.ioa.ac.cn; sfyan@ieee.org).

Hongming Zhang is with the School of Information and Communication Engineering, Beijing University of Posts and Telecommunications, Beijing 100876, China (e-mail: zhanghm@bupt.edu.cn).

Lie-Liang Yang and Lajos Hanzo are with the Department of Electronics and Computer Science, University of Southampton, Southampton SO17 1BJ, U.K. (e-mail: lly@ecs.soton.ac.uk; lh@ecs.soton.ac.uk).

L. Hanzo would like to acknowledge the financial support of the European Research Council's Advanced Fellow Grant QuantCom (Grant No. 789028)

II, our system model is illustrated. Section III introduces both the AMP algorithm and the MMSE-DAMPD. Our simulation results are provided in Section IV, while our conclusions are summarized in Section V.

II. System Model

TABLE I
Summary of Literature Review on OFDM-IM Detection

Contributions	**Our scheme**	[4]	[12]	[7]	[2], [10]
Generalized OFDM-IM	✓		✓	✓	✓
Sparsity	✓	✓	✓	✓	✓
AMP	✓	✓	✓	✓	
Damping	✓		✓	✓	
MMSE Denoiser	✓				
RMSE Performance	✓				

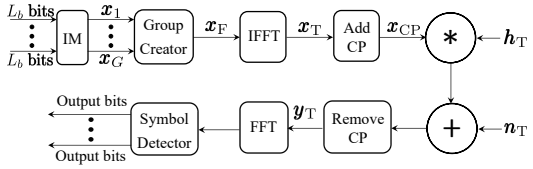

Fig. 1. Illustration of the IM-OFDM system

Consider an OFDM system having M subcarriers, which are divided into G groups, yielding $m = M/G$ subcarriers in each group. Correspondingly, as shown in Fig. 1, L_b bits are first split into G groups, each containing $L = L_b/G = L_1 + L_2$ bits. In each group, L_1 bits are mapped to an index symbol based on an index mapper $\mu_1 : \mathbb{B}^{L_1} \to \mathcal{Z}$, where $\mathcal{Z}$ contains $C = 2^{L_1}$ subsets and each subset is generated by selecting k active indices from m indices. Therefore, we have $L_1 = \log_2 C = \left\lfloor \log_2 \binom{m}{k} \right\rfloor$. In the gth group, L_1 bits are mapped into a subset of $\mathcal{Z}$ and the set of index symbols is denoted by $\mathcal{I}_g \leftrightarrow \mathcal{Z}_c \subset \mathcal{Z}$, where $\mathcal{Z}_c$ denotes the cth subset of $\mathcal{Z}$. Furthermore, we employ an APM mapper $\mu_2 : \mathbb{B}^{\log_2 Q} \to \mathcal{A}$ to map $L_2 = k \log_2 Q$ bits onto k APM symbols in the normalized constellation set $\mathcal{A} \triangleq \{a_1, \ldots, a_Q\}$ of a Q-ary quadrature amplitude modulation (QAM)/phase-shift keying (PSK) scheme. Let us denote the APM symbols in the gth group by $\boldsymbol{x}_g^d = [x_0^d, \ldots, x_{k-1}^d]^T$, thus we can attain a symbol vector $\boldsymbol{x}_g = \boldsymbol{\Upsilon}_{\mathcal{I}_g} \boldsymbol{x}_g^d$, where $\boldsymbol{x}_g = [x_0, \ldots, x_{m-1}]^T$ and $\boldsymbol{\Upsilon}_{\mathcal{I}_g}$ is an $(m \times k)$-element mapping matrix formed according to $\mathcal{I}_g$. Given the subcarrier activation scheme, the rate is formulated as $R = L/m = \left(\left\lfloor \log_2 \binom{m}{k} \right\rfloor + k \log_2 Q\right)/m$ bits/s/Hz [10].

As shown in Fig. 1, the symbols in all the G groups are combined to form the FD symbols expressed as $\boldsymbol{x}_\mathrm{F} = [x_{\mathrm{F},0}, x_{\mathrm{F},1}, \ldots, x_{\mathrm{F},M-1}]^T$. After the M-point inverse fast Fourier transform (IFFT) and inserting a cyclic prefix (CP), we obtain the transmitted baseband signals $\boldsymbol{x}_\mathrm{cp}$.

Overall a frequency-selective Rayleigh fading channel having L_h taps is considered, whose channel impulse response (CIR) is denoted as $\boldsymbol{h} = [h_0, h_1, \ldots, h_{L_\mathrm{h}-1}]^T$, and the CIR-taps are independent and identically distributed (i.i.d.) random variables obeying the distribution $\mathcal{CN}(0, 1/L_\mathrm{h})$. Then, upon assuming $L_\mathrm{cp} \geq L_\mathrm{h}$, after removing the CP and the FFT-based demodulation, the received FD symbol vector in the gth group can be written as

$$\boldsymbol{y}_g = \bar{\boldsymbol{H}}_g \boldsymbol{x}_g + \bar{\boldsymbol{n}}_g, \quad g = 1, 2, \ldots, G, \tag{1}$$

where $\bar{\boldsymbol{n}}_g$ is the FD noise vector of the gth group. Furthermore, it can be readily shown that $\bar{\boldsymbol{H}}_g = \mathrm{diag}\{\bar{h}_{g,0}, \ldots, \bar{h}_{g,m-1}\}$. According to [2], we have $\bar{h}_{g,i} \sim \mathcal{CN}(0, 1)$ and $\bar{n}_{g,i} \sim \mathcal{CN}(0, N_0)$, $\forall g, i$. As a result, the average SNR per symbol can be evaluated as $\gamma_s \triangleq \mathbb{E}[\|\boldsymbol{x}_g\|_2^2]/\mathbb{E}[\|\bar{\boldsymbol{n}}_g\|_2^2] = k/(mN_0)$. Furthermore, if the candidates in Ω are independent and equiprobable, the optimum detector is the maximum likelihood (ML) detector, which is defined by the following the optimization problem

$$\boldsymbol{x}_g^\mathrm{ML} = \arg\min_{\boldsymbol{x}_g \in \Omega} \left\{ \left\| \boldsymbol{y}_g - \bar{\boldsymbol{H}}_g \boldsymbol{x}_g \right\|_2^2 \right\}. \tag{2}$$

III. Damping AMP Aided Detection relying on an MMSE Denoiser

However, the complexity of the optimal ML detector becomes excessive, if the number of bits L per symbol is high. To mitigate this problem in this section, we propose a low-complexity detector termed as MMSE-DAMPD by exploiting the sparse structure of the FD symbols at the receiver. We continue by first discussing the conventional AMP OFDM-IM receiver, followed by the MMSE denoiser. Finally, we detail the MMSE-DAMPD.

A. Conventional AMP Algorithm

The operation of the AMP commences from $\boldsymbol{x}_g^{[0]} = \boldsymbol{0}$ and $\boldsymbol{z}_g^{[0]} = \boldsymbol{y}_g$ and proceeds iteratively as follows [11]:

$$\check{\boldsymbol{x}}_g^{[t]} = \boldsymbol{x}_g^{[t]} + \bar{\boldsymbol{H}}_g^H \boldsymbol{z}_g^{[t]}, \tag{3}$$

$$\boldsymbol{x}_g^{[t+1]} = \eta(\check{\boldsymbol{x}}_g^{[t]}; \sigma_{g,t}), \tag{4}$$

$$\boldsymbol{z}_g^{[t+1]} = \boldsymbol{y}_g - \bar{\boldsymbol{H}}_g \boldsymbol{x}_g^{[t+1]} + \frac{\boldsymbol{z}_g^{[t]}}{2m} \nabla \eta(\check{\boldsymbol{x}}_g^{[t]}; \sigma_{g,t}), \tag{5}$$

where $\boldsymbol{x}_g^{[t]} = [x_{g,0}^{[t]}, \ldots, x_{g,m-1}^{[t]}]^T$ is the estimate of $\boldsymbol{x}_g$ at iteration t. In the conventional AMP algorithm, the component-wise complex soft threshold denoiser $\eta(\boldsymbol{u}; \sigma)$ of [13] is used, when the *a priori* distribution of $\boldsymbol{x}_g$ is unknown.

Let us assume that $k, m \to \infty$ and the marginal distribution of $\boldsymbol{x}_g$ converges to p_{X_g}. Then, the performance of the AMP receiver can be predicted according to the state evolution function of [11]

$$\sigma_{g,t+1}^2 = \mathbb{E}\left[\left| \eta(X_g + \sigma_{g,t} Z; \sigma_{g,t}) - X_g \right|^2 \right] + N_0, \tag{6}$$

where $\sigma_{g,t}$ characterizes the RMSE of $\check{\boldsymbol{x}}_g^{[t]}$ at iteration t, and the expectation is taken with respect to the independent random variables of $Z \sim \mathcal{CN}(0, 1)$ and $X_g \sim p_{X_g}$.

B. MMSE Denoiser in MMSE-DAMPD

One of our main objectives is to exploit the statistical characteristics of the transmitted symbols for improving the detection performance. By applying this approach to OFDM-IM, we propose an AMP detector amalgamated with an MMSE denoiser, which is detailed below. Note that since the received signals of different groups are processed similarly,

for the sake of simplicity, we omit the group subscript g throughout this section.

Bearing in mind that the elements in $\boldsymbol{x}$ can be zero or non-zero, we have $\Pr(x_i \neq 0) = \rho$, $\forall i \in \{i = 0, \ldots, m-1\} = \mathcal{M}$, where $\rho = k/m$ is the signal sparsity. According to the characteristics of IM and APM modulation, the PDF of the entries of $\boldsymbol{x}$ can be formulated as

$$p_X(x_i^{[t]}) = (1-\rho)\delta_0 + \rho \bar{p}_X(x_i^{[t]}), \tag{7}$$

where δ_0 denotes the point mass measure at 0 and $\bar{p}_X(x_i^{[t]}) = \sum_{q=1}^{Q} \delta(x_i^{[t]} - a_q)/Q, \quad i = 0, \ldots, m-1$. Based on (6), the MMSE denoiser can be formulated as

$$\eta_{\text{MMSE}}(\check{x}_i^{[t]}; \sigma_t) = \mathbb{E}\left[X | \check{X}^{[t]} = \check{x}_i^{[t]}\right], \tag{8}$$

where $\check{X} = X + \sigma_t Z$ is a random variable having a mixed distribution. Let us omit the superscript $[t]$ and subscript i for notation simplicity. Then, based on the Bayesian rule, the conditional expectation can be expressed as

$$\begin{aligned}\mathbb{E}[X|\check{X} = \check{x}] &= \int x \frac{p_X(x)}{p_{\check{X}}(\check{x})} p_{\check{X}|X}(\check{x}|x) dx \\ &= \int x \frac{p_X(x)}{\pi\sigma^2 p_{\check{X}}(\check{x})} \exp\left(-\frac{|\check{x}-x|^2}{\sigma^2}\right) dx. \end{aligned} \tag{9}$$

Specifically, it may be readily shown that $p_{\check{X}|X}(\check{x}|X=0) = p_W(\check{x})$, where $W = \sigma Z$, and $p_{\check{X}|X}(\check{x}|X \neq 0) = p_Y(\check{x})$ with $Y = \underline{X} + W$ and $\underline{X} \sim \bar{p}_{\underline{X}}(\underline{x})$. In more detail, we have

$$p_{\check{X}|X}(\check{x}|X=0) = \frac{1}{\pi\sigma^2} \exp\left(-\frac{|\check{x}|^2}{\sigma^2}\right), \tag{10}$$

$$\begin{aligned} p_Y(\check{x}) &= \int p_{\underline{X}}(\check{x} - \omega) p_W(\omega) d\omega \\ &= \sum_{q=1}^{Q} \frac{1}{\pi\sigma^2 Q} \exp\left(-\frac{|\check{x} - a_q|^2}{\sigma^2}\right). \end{aligned} \tag{11}$$

Furthermore, upon substituting (10) and (11) into (7), we can show that the PDF of $\check{x}$ can be formulated as

$$p_{\check{X}}(\check{x}) = \frac{1-\rho}{\pi\sigma^2} \exp\left(-\frac{|\check{x}|^2}{\sigma^2}\right) + \sum_{q=1}^{Q} \frac{\rho}{\pi\sigma^2 Q} \exp\left(-\frac{|\check{x}-a_q|^2}{\sigma^2}\right). \tag{12}$$

Based on (7) and (12), after evaluating the integral of (9), the MMSE denoiser, i.e. the conditional expectation in (8) can be expressed as

$$\mathbb{E}[X|\check{X} = \check{x}] = \frac{u(\check{x})}{v(\check{x})}, \tag{13}$$

where $u(\check{x})$ and $v(\check{x})$ are given by

$$u(\check{x}) = \frac{\rho}{Q} \sum_{q=1}^{Q} a_q \exp\left(-\frac{|\check{x}-a_q|^2}{\sigma^2}\right), \tag{14}$$

$$v(\check{x}) = (1-\rho)\exp\left(-\frac{|\check{x}|^2}{\sigma^2}\right) + \sum_{q=1}^{Q} \frac{\rho}{Q} \exp\left(-\frac{|\check{x}-a_q|^2}{\sigma^2}\right). \tag{15}$$

The divergence $\nabla\eta_{\text{MMSE}}(\check{x})$ of the MMSE denoiser $\eta_{\text{MMSE}}(\check{x})$ can be formulated as

$$\nabla\eta_{\text{MMSE}}(\check{x}) = \frac{1}{\sigma^2}\text{Var}(X|\check{X} = \check{x}), \tag{16}$$

while the conditional moment $\mathbb{E}[|X|^2|\check{X} = \check{x}]$ can be expressed as

$$\mathbb{E}[|X|^2|\check{X} = \check{x}] = \int |x|^2 \frac{p_X(x)}{p_{\check{X}}(\check{x})} p_{\check{X}|X}(\check{x}|x) dx = \frac{\xi(\check{x})}{v(\check{x}),} \tag{17}$$

where $v(\check{x})$ is given in (15), and $\xi(\check{x})$ is

$$\xi(\check{x}) = \frac{\rho}{Q} \sum_{q=1}^{Q} |a_q|^2 \exp\left(-\frac{|\check{x}-a_q|^2}{\sigma^2}\right). \tag{18}$$

Hence, upon substituting the results into (16), the divergence of the MMSE denoiser is expressed as

$$\nabla\eta_{\text{MMSE}}(\check{x}) = \frac{1}{\sigma^2}\left[\frac{\xi(\check{x})}{v(\check{x})} - \left|\frac{u(\check{x})}{v(\check{x})}\right|^2\right], \tag{19}$$

where $u(\check{x})$ can be obtained from (14). Consequently, the divergency $\nabla\eta_{\text{MMSE}}(\boldsymbol{u}; \sigma)$ required by (5) can be obtained.

C. MMSE Denoiser Based Damping-assisted AMP-aided Detection

In order to reduce the number of errors at the beginning of iterations and also to minimize the number of iterations in the iterative detection process, at the first stage, the observation vector $\boldsymbol{y}$ is firstly processed by the linear minimum mean square error (LMMSE) detector, yielding

$$\bar{\boldsymbol{x}} = \left(\bar{\boldsymbol{H}}^H \bar{\boldsymbol{H}} + \frac{1}{\gamma_s}\boldsymbol{I}_m\right)^{-1} \bar{\boldsymbol{H}}^H \boldsymbol{y}, \tag{20}$$

where $\bar{\boldsymbol{x}} = [\bar{x}_0, \ldots, \bar{x}_{m-1}]^T \in \mathbb{C}^{m\times 1}$ is a soft estimate of $\boldsymbol{x}$.

Then, we set $\boldsymbol{x}^{[0]} = \bar{\boldsymbol{x}}$, and the enhanced estimation $\tilde{\boldsymbol{x}} = [\tilde{x}_0, \ldots, \tilde{x}_{m-1}]^T$ of $\boldsymbol{x}$ is carried out by the MMSE-DAMPD using T iterations during the second stage, as detailed below.

As for the operation of the MMSE-DAMPD, the reliabilities of index symbols can be quantified by sorting the amplitudes of the elements in $\tilde{\boldsymbol{x}}$ in descending order as [10]

$$\{i_0, \ldots, i_{m-1}\} \quad \text{corresponding to} \, |\tilde{x}_{i_0}|^2 \geqslant \ldots \geqslant \left|\tilde{x}_{i_{m-1}}\right|^2, \tag{21}$$

where we have $i_j \in \mathcal{M}$ for $j = 0, \ldots, m-1$ and $i_j \neq i_q$ for any $j \neq q$. Then, after picking the first k elements in $\{i_0, \ldots, i_{m-1}\}$ and sorting their indices in ascending order, we obtain the estimated index set $\mathcal{Z}_E \triangleq \{b_0, b_1, \ldots, b_{k-1}\}$, where $b_j \in \mathcal{M}$, $\forall j \in \{0, \ldots, k-1\}$. Furthermore, by identifying the k elements having the highest amplitudes in $\tilde{\boldsymbol{x}}$, the preliminary estimate $\tilde{\boldsymbol{x}}^d$ of the conventional APM data symbols can expressed as $\tilde{\boldsymbol{x}}^d = [\tilde{x}_{b_0}^d, \tilde{x}_{b_1}^d, \ldots, \tilde{x}_{b_{k-1}}^d]^T$. Therefore, the estimated APM symbols in $\hat{\boldsymbol{x}}^d = [\hat{x}_0^d, \hat{x}_1^d, \ldots, \hat{x}_{k-1}^d]^T$ can be obtained by applying simple symbol-by-symbol ML detection, formulated as

$$\hat{x}_i^d = \arg\min_{a_q \in \mathcal{A}} |\tilde{x}_{b_i}^d - a_q|^2, \quad i = 0, \ldots, k-1. \tag{22}$$

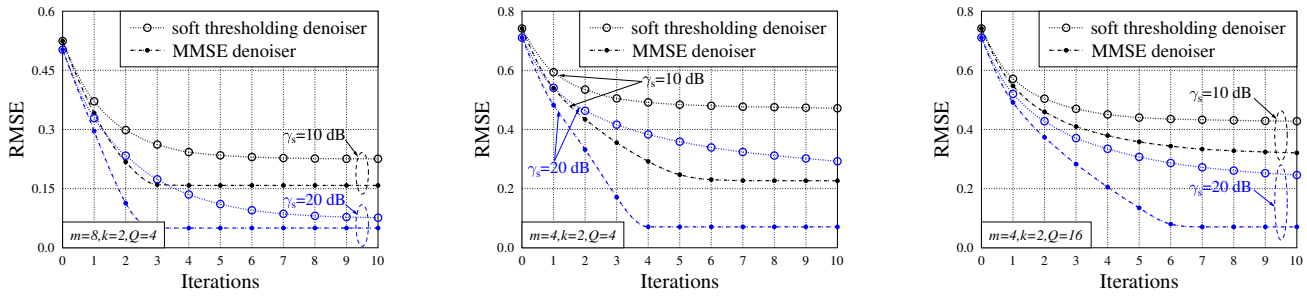

Fig. 2. RMSE performance of the soft thresholding denoiser and the MMSE denoiser operating at (a) $(m = 8, k = 2, Q = 4)$ (b) $(m = 4, k = 2, Q = 4)$ (c) $(m = 4, k = 2, Q = 16)$ and γ_s =10 dB or 20 dB.

Then MMSE-DAMPD then enters the third stage of detecting the index symbols, we define indicator vectors $\boldsymbol{u}_{\mathcal{Z}_c} = [u_{c,0}, u_{c,1}, \ldots, u_{c,m-1}]^T$ for $c = 1, 2, \ldots, C$ and the check vector $\check{\boldsymbol{u}}_{\mathcal{Z}_E} = [\check{u}_0, \check{u}_1, \ldots, \check{u}_{m-1}]^T$ based on the index dictionary set $\mathcal{Z}$ and the estimation set $\mathcal{Z}_E$, respectively. Moreover, we have $u_{c,i} = \mathbb{I}_{(i\in\mathcal{Z}_c)}$ and $\check{u}_j = \mathbb{I}_{(j\in\mathcal{Z}_E)}$, where $i, j = 0, 1, \ldots, m-1$. The candidates can be obtained by finding N subsets $\mathcal{Z}_{i_j}$ in $\mathcal{Z}$ that minimize $\|\boldsymbol{u}_{\mathcal{Z}_{i_j}} - \check{\boldsymbol{u}}_{\mathcal{Z}_E}\|_0$, where we have $i_j \in \{1, 2, \ldots, C\}$ for $j = 1, \ldots, N$. Thus we have $\tilde{\mathcal{Z}} = \{\mathcal{Z}_{i_1}, \mathcal{Z}_{i_2}, \ldots, \mathcal{Z}_{i_N}\} \subset \mathcal{Z}$. Explicitly, if the candidate is detected correctly at this step, we have $\boldsymbol{u}_{\mathcal{Z}_c} = \check{\boldsymbol{u}}_{\mathcal{Z}_E}$. This implies that there is only a single subset in $\tilde{\mathcal{Z}}$, which satisfies that $\tilde{\mathcal{Z}}_{i_1} = \mathcal{Z}_E$. Consequently, based on the candidate space $\tilde{\mathcal{Z}}$, which is regarded as *a priori* information for the ensuing detection of the activated symbols, the estimation of active indices $\mathcal{I}$ can be formulated as

$$\hat{\mathcal{I}} = \underset{\mathcal{Z}_{i_j}\in\tilde{\mathcal{Z}}}{\arg\max} \|\mathrm{diag}(\boldsymbol{u}_{\mathcal{Z}_{i_j}})\tilde{\boldsymbol{x}}\|_2^2. \tag{23}$$

The performance of the AMP algorithm may be poor for non-i.i.d zero-mean complex Gaussian sensing matrices. To mitigate this problem, a damping strategy is conceived for the conventional AMP algorithm, in which the iterative equations (4) and (5) are modified to

$$\boldsymbol{x}^{[t+1]} = \theta\eta(\check{\boldsymbol{x}}^{[t]}; \sigma_t) + (1-\theta)\boldsymbol{x}^{[t]}, \tag{24}$$

$$\boldsymbol{z}^{[t+1]} = \boldsymbol{y} - \bar{\boldsymbol{H}}\boldsymbol{x}^{[t+1]} + \theta\frac{\boldsymbol{z}^{[t]}}{2m}\nabla\cdot\eta(\check{\boldsymbol{x}}^{[t]}; \sigma_t), \tag{25}$$

respectively, where θ denotes the damping factor.

Remark 1: At the third stage of the MMSE-DAMPD, by searching in $\mathcal{Z}$, we first obtain N active index combinations that satisfy the condition that $\boldsymbol{u}_{\mathcal{Z}_{i_j}}$ and $\check{\boldsymbol{u}}_{\mathcal{Z}_E}$ have the least number of different elements at the same indices. Furthermore, we calculate the total symbol energy of k elements in $\tilde{\boldsymbol{x}}$ corresponding to the N-selected active index combinations. Finally, $\hat{\mathcal{I}}$ is obtained by finding the highest energy value. However, the estimation of active indices $\hat{\mathcal{I}}_{\mathrm{LLR}}$ is calculated by finding the k highest LLR values in the LLRD. If $\hat{\mathcal{I}}_{\mathrm{LLR}} \notin \mathcal{Z}$, i.e. $\hat{\mathcal{I}}_{\mathrm{LLR}}$ represents an unused index combination (corresponding to the case of $N \neq 1$ in MMSE-DAMPD), the output bits $\hat{L}_1$ are all erroneous [8]. Since the MMSE-DAMPD further processes the unused index combinations theoretically, it has a better BER performance than the LLRD.

D. Complexity Analysis

First, the ML detection complexity of each group is given by searching all the possible candidates in Ω as well as the matrix calculation based on (2). Therefore the detection complexity order is given by

$$\mathcal{O}\left[m(m+m)2^L\right] = \mathcal{O}\left(m^2 2^{L+1}\right), \tag{26}$$

which represents an exponential growth with the number of bits L. Thus, the ML detector becomes excessively complex, if the value of L is relatively high. Moreover, the complexity of the LLRD is on the order of $(3Q+2)m$ per group [8].

According to our analysis in Section III-C, the LMMSE detection complexity is on the order of $\mathcal{O}(4m)$, while the MMSE-DAMPD complexity order without the expectations is given by $\mathcal{O}(3mT)$. Furthermore, the MMSE denoiser complexity is on the order of $\mathcal{O}[(4Q+4)mT]$ and the divergence of the denoiser complexity is given by $\mathcal{O}(2mT)$. Therefore, it can be readily shown that the overall complexity is on the order of

$$\mathcal{O}\left[4m + (4Q+9)mT\right], \tag{27}$$

since the components of (22) and (23) have been calculated in (14).

IV. Numerical Results

In this section, our simulation results are provided for characterizing the performance of the proposed MMSE denoiser and MMSE-DAMPD. The number of CIR-taps, the tolerance parameter and the damping factor are set as $L_{\mathrm{h}} = 10$, $\epsilon = 10^{-12}$ and $\theta = 0.2$, respectively. We assume an OFDM-IM system having $M = 256$ subcarriers and a CP-length of $L_{\mathrm{cp}} = 16$. For the sake of comparison, ζM subcarriers are employed for transmitting Q-ary QAM symbols in the classic OFDM systems, yielding a transmission rate of $\zeta \log_2 Q$ bits/s/Hz, corresponding to different SAPs in OFDM-IM systems, as detailed in Table II.

According to Section III-A and the constellation set $\mathcal{A}$, beginning with $\sigma_{g,0} = \rho/\delta + N_0$, the RMSE performances of the soft thresholding denoiser and of the MMSE denoiser in the cases of different system parameters are compared in Fig. 2. The maximum number of iterations is $T = 10$. Based on the results, we have the following observations. Firstly, the RMSE performance of the MMSE denoiser is

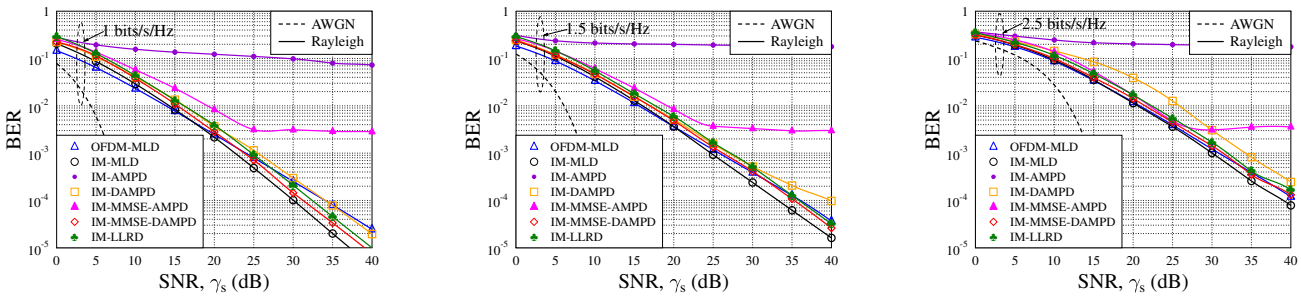

Fig. 3. BER versus SNR for the classic OFDM using MLD and OFDM-IM using MLD, AMPD, DAMPD, MMSE-AMPD, MMSE-DAMPD and LLRD when communicating over an $L_h = 10$-path Rayleigh fading channel, and operating at (a) 1bits/s/Hz (b) 1.5bits/s/Hz (c) 2.5bits/s/Hz

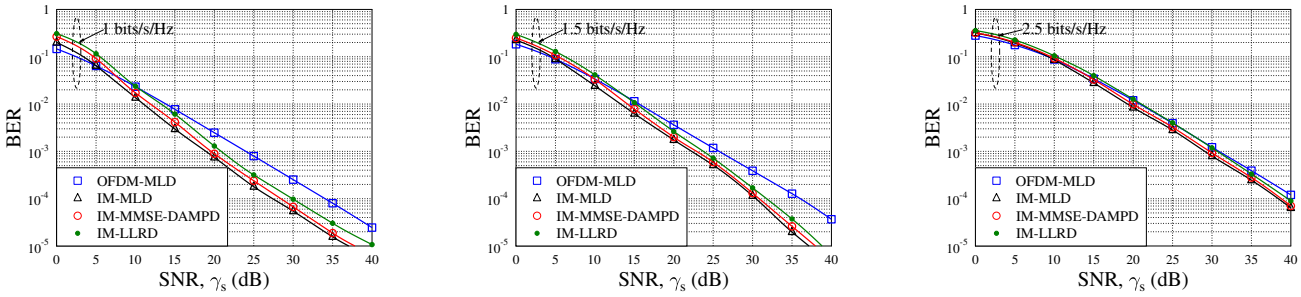

Fig. 4. BER versus SNR for the classic OFDM using MLD and interleaved OFDM-IM using MLD, MMSE-DAMPD, and LLRD when communicating over an $L_h = 10$-path Rayleigh fading channel, and operating at (a) 1bits/s/Hz (b) 1.5bits/s/Hz (c) 2.5bits/s/Hz.

TABLE II
SIMULATIONS PARAMETERS

Rate R in bits/s/Hz	System Parameters (m, k, Q)	Ratio of Data Subcarriers ζ
1	$(8, 2, 4)$	0.5
1.5	$(4, 2, 4)$	0.75
2.5	$(4, 2, 16)$	0.625

better than that of the soft thresholding denoiser. This is because the MMSE denoiser exploits the *a priori* distribution of the transmitted symbol vector $\boldsymbol{x}_g$. Secondly, for a given γ_s and when the RMSE becomes stable, our proposed MMSE denoiser significantly outperforms the classic soft thresholding based denoiser. This observation can be explained by the fast that the MMSE denoiser minimizes the RMSE generated by the reconstruction process at every iteration. Thirdly, as seen in Fig. 2 (a) and Fig. 2 (b), when the values of Q and δ are fixed, the lower sparsity ρ leads to a better RMSE performance. This is because the AMP algorithms can obtain a higher successful reconstruction probability, as the sparsity increases. Furthermore, the RMSE performance of the MMSE denoiser shown in Fig. 2 (c) is slightly worse than that shown in Fig. 2 (b). According to (16) and (19), since higher divergency $\nabla\eta_{\text{MMSE}}(\boldsymbol{u};\sigma)$ can be attained for $Q = 16$, the attainable RMSE performance degrades, when a higher-order modulation scheme is used.

In Fig. 3, the BER performance of the proposed MMSE-DAMPD is investigated at different attainable rates where OFDM operating in additive white Gaussian noise (AWGN) channels is used as a benchmark. The maximum number of iterations is $T = 6$. Based on Fig. 3, we have the following observations. Firstly, for a given rate, we observe that the BER performance of the OFDM-IM systems using the MMSE denoiser based AMP detector (MMSE-AMPD) is significantly better than those employing the conventional AMP detector (AMPD). This is because MMSE-AMPD attains a better RMSE. Secondly, the OFDM-IM systems using our damping-assisted detectors are capable of achieving better BER performances than that using non-damping detectors. This is because the convergence performance of the AMP algorithm is improved with the aid of our damping strategy in the face of practical sensing matrixes. The above analysis can also explain why the BER performance of AMPD is the worst among the different detectors considered. Moreover, when the transmission rate R is fixed, our MMSE-DAMPD significantly outperforms the DAMPD, and a satisfactory BER performance can be attained for MMSE-DAMPD. Furthermore, observe in Fig. 3 (a) and Fig. 3 (b) for BER values of 10^{-4}, and in Fig. 3 (c) for 10^{-3}, that the BER performance of MMSE-DAMP is about 1 dB better than that of the LLRD. This observation can be explained with the aid of the analytical results shown in Section III-C. Explicitly, we define the percentage of the number of unused combinations $\eta = [\binom{m}{k} - C]/\binom{m}{k}$. Since η is equal to 42.9% for $(m = 8, k = 2)$ and 33.3% for $(m = 4, k = 2)$, which are higher than the 8.6% employed in [8], the receiver is more likely to decide on a catastrophic set of active indices. A further active index detection stage based on the set of unused index combinations is employed by MMSE-DAMPD, rather than simply deciding that the corresponding bits are erroneous. As a benefit, the MMSE-

DAMPD is capable of achieving a lower BER than the LLRD. Finally, observe from Fig. 3 (b) and Fig. 3 (c) that better BER performance can be achieved for lower APM constellation sizes, which have an increased Euclidean minimum distance.

To further demonstrate the efficiency of our proposed scheme, we employ a subcarrier-level interleaved OFDM-IM that gleans additional frequency diversity [10]. The BER performances of OFDM-MLD and OFDM-IM using different detectors are compared in Fig. 4. Firstly, for a given rate, we observe from this figure that the BER performance of the interleaved OFDM-IM is better than that of OFDM in the region of $\gamma_s > 5$ dB. This trend can be explained by the fact that the interleaver increases the Euclidean distances among the modulated OFDM-IM symbols. Moreover, for a BER value of 10^{-4}, the MMSE-DAMPD provides approximately 1 dB better BER performance than the LLRD, which is consistent with the observations from Fig. 3.

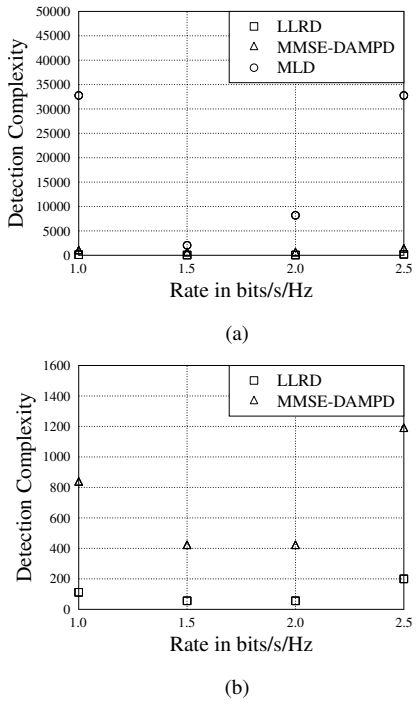

Fig. 5. Rate versus detection complexity for the OFDM-IM using LLRD, MMSE-DAMPD, and MLD.

In Fig. 5, we compare the detection complexity of LLRD, MMSE-DAMPD and MLD, where Fig. 5 (b) represents the detail view of Fig. 5 (a). The parameters corresponding to $R = 2$ bits/s/Hz are $(m = 4, k = 3, Q = 4)$. Observe that the LLRD and MMSE-DAMPD have a much lower complexity than the MLD. This can be explained as follows. Firstly, as seen in Fig. 2, a faster and also more accurate convergence is achieved by the MMSE denoiser. Secondly, the AMP algorithm relies on low-complexity linear operations in each of the iterations. Moreover, based on (2) and (22), it may be observed that the MMSE-DAMPD is a symbol-by-symbol detection scheme, while the MLD carries out joint group-based detection. Finally, based on Fig. 3, Fig. 4 and Fig. 5, we may conclude that the MMSE-DAMPD achieves a better BER performance than the LLRD at the cost of a slightly higher complexity.

V. Conclusions

An AMP-assisted OFDM-IM detection framework has been investigated. By exploiting the PDF of transmitted symbols and the classic Bayesian approach, an MMSE denoiser has been proposed for AMP detection. As shown by our theoretical analysis, the proposed MMSE denoiser provides estimates having the minimum RMSE at each and every iteration. Our simulation results have shown that the MMSE denoiser attains both a better RMSE and a better convergence performance than the soft thresholding denoiser. Moreover, new MMSE-AMPD schemes have been proposed for reducing the detection complexity. Furthermore, a novel damping strategy has been conceived for AMP detectors. Simulation results have shown that compare to non-damping detectors, the damping AMP detectors which has improved the BER performance. The proposed MMSE-DAMPD can attains a good BER performance at a low complexity.

References

[1] R. Rajashekar, C. Xu, N. Ishikawa, L. Yang, and L. Hanzo, "Subcarrier subset selection-aided transmit precoding achieves full-diversity in index modulation," *IEEE Transactions on Vehicular Technology*, vol. 68, no. 11, pp. 11 031–11 041, 2019.

[2] H. Zhang, L. L. Yang, and L. Hanzo, "Compressed sensing improves the performance of subcarrier index-modulation-assisted OFDM," *IEEE Access*, vol. 4, pp. 7859–7873, 2016.

[3] C. Masouros and L. Hanzo, "A scalable performancecomplexity tradeoff for constellation randomization in spatial modulation," *IEEE Transactions on Vehicular Technology*, vol. 66, no. 3, pp. 2834–2838, 2017.

[4] H. Zhang, Z. Sui, E. Basar, L.-L. Yang, and L. Hanzo, "Performance evaluation of index modulation with single subcarrier activation," in *2021 IEEE Wireless Communications and Networking Conference (WCNC)*, 2021, pp. 1–7.

[5] H. Zhang, L. L. Yang and L. Hanzo, "LDPC-coded index-modulation aided OFDM for in-vehicle power line communications," in *2016 IEEE 83rd Vehicular Technology Conference (VTC Spring)*, May 2016, pp. 1–5.

[6] S. Lu, M. El-Hajjar, and L. Hanzo, "Two-dimensional index modulation for the large-scale multi-user mimo uplink," *IEEE Transactions on Vehicular Technology*, vol. 68, no. 8, pp. 7904–7918, 2019.

[7] L. Wei, J. Zheng, and Q. Liu, "Approximate message passing detector for index modulation with multiple active resources," *IEEE Transactions on Vehicular Technology*, vol. 68, no. 1, pp. 972–976, 2019.

[8] E. Başar, Ü. Aygölü, E. Panayırcı, and H. V. Poor, "Orthogonal frequency division multiplexing with index modulation," *IEEE Transactions on signal processing*, vol. 61, no. 22, pp. 5536–5549, 2013.

[9] J. Crawford and Y. Ko, "Low complexity greedy detection method with generalized multicarrier index keying OFDM," in *2015 IEEE 26th Annual International Symposium on Personal, Indoor, and Mobile Radio Communications (PIMRC)*, 2015, pp. 688–693.

[10] H. Zhang, C. Jiang, L.-L. Yang, E. Basar, and L. Hanzo, "Linear precoded index modulation," *IEEE Transactions on Communications*, vol. 67, no. 1, pp. 350–363, 2018.

[11] D. L. Donoho, A. Maleki, and A. Montanari, "Message-passing algorithms for compressed sensing," *Proceedings of the National Academy of Sciences*, vol. 106, no. 45, pp. 18 914–18 919, 2009.

[12] Q. Shi, N. Wu, H. Wang, X. Ma, and L. Hanzo, "Factor graph based message passing algorithms for joint phase-noise estimation and decoding in OFDM-IM," *IEEE Transactions on Communications*, vol. 68, no. 5, pp. 2906–2921, 2020.

[13] A. Maleki, L. Anitori, Z. Yang, and R. G. Baraniuk, "Asymptotic analysis of complex lasso via complex approximate message passing (CAMP)," *IEEE Transactions on Information Theory*, vol. 59, no. 7, pp. 4290–4308, 2013.